ELSEVIER

Journal of Organometallic Chemistry 637–639 (2001) 445–462

Journal of Organometallic Chemistry

www.elsevier.com/locate/jorganchem

Electron acceptors of the fluorene series☆. Part 12. 9-(Metalloceneylidene)nitrofluorene derivatives of Fc–NF, NF–Fc–NF, and NF–Rc–NF types, and the vinylogues Fc–π–NF: synthesis, characterisation, intramolecular charge transfer, redox properties and X-ray structures for three fluorene–ferrocene derivatives

Dmitrii F. Perepichka [a,b], Igor F. Perepichka [a,*], Anatolii F. Popov [a], Martin R. Bryce [b,*], Andrei S. Batsanov [b], Antony Chesney [b], Judith A.K. Howard [b], Nikolai I. Sokolov [c]

[a] *L.M. Litvinenko Institute of Physical Organic and Coal Chemistry, National Academy of Sciences of Ukraine, Donetsk 83114, Ukraine*
[b] *Department of Chemistry, University of Durham, Durham DH1 3LE, UK*
[c] *Laboratory of Holography, Natural Faculty, University 'Kyivo-Mogilyans'ka Academy', Kiev 04145, Ukraine*

Received 25 January 2001; received in revised form 16 March 2001; accepted 20 March 2001

Abstract

Reaction of ferrocenecarboxaldehyde **13** and its vinylogue, (*E,E*)-1-ferrocenyl-4-formyl-1,3-butadiene (**16**), with nitrofluorenes as CH-acids, results in push–pull compounds of the type Fc–π–fluorene (**8a–g**, **12a–e**). Similar reaction with bifunctional ferrocene and ruthenocene dicarboxaldehydes results, depending on the fluorene structure, in the products of mono- or di-condensation, OHC–Fc–CH=fluorene (**11d,e**) or fluorene=CH–Fc–CH=fluorene and fluorene=CH–Rc–CH=fluorene (**9a–c**, **10a–c**). Intramolecular charge transfer (ICT) in compounds **8** results in lowering the rotation barrier around the CH=fluorene double bond and easy *E–Z* isomerisation in solution. Cyclic voltammetry (CV) experiments show a reversible single-electron oxidation of Fc–CH=fluorenes (**8**) yielding the cation and two reversible single-electron reduction waves yielding the radical anion and dianion (for **8a–e**) which merge into one two-electron reduction wave for **8f–h**. ICT was also manifested in the electron absorption spectra of **8–12**, and energies of ICT (as well as reduction potentials in CV) were found to display excellent correlation ($r \geq 0.99$) with Hammett-type substituents constants (σ_p^-) in the fluorene moiety. Compounds **8–12** show solvatochromism [**8a**: $\lambda_{ICT} = 604.5$ nm (acetonitrile), 622.5 nm (1,2-dichloroethane)], with, however, no quantitative regularities for 10 solvents of different polarity. Bathochromic shifts of 40–83 nm and an increase in the intensity of ICT bands were observed with lengthening of the π-bridge between ferrocene and fluorene moieties (**8** → **12**) whereas substitution of the ferrocene unit in **9** by the ruthenocene unit (**10**) resulted to a hypsochromic shift of ca. 100 nm due to decreasing donor ability of the latter metallocene fragment. Acceptor **8a** was found to sensitise the photoconductivity of poly-*N*-(2,3-epoxypropyl)carbazole showing moderate holographic response of the materials. Molecular and crystal structures for ferrocene derivatives **8a**, **8g**, and **11d** were determined by single-crystal X-ray diffraction. Tetranitro derivative **8a** shows substantial distortion, caused by steric repulsion between the nitro groups in positions 4 and 5, which precludes the formation of stacks, and pairs of fluorene moieties contact face-to-face (interplanar distance 3.8 Å). In di- and trinitro derivatives **8g** and **11d** the fluorene moieties are more planar and their crystal packing motifs are similar: fluorene moieties form good stacks, parallel to the *x*-axis in **8g** and the *y*-axis in **11d**, with interplanar separations between fluorene moieties of 3.35–3.36 Å for **8g** and alternate separations of 3.52 and 3.55 Å for **11d**.

Keywords: Ferrocene; Push–pull compounds; Cyclic voltammetry; Intramolecular charge transfer; Electron acceptors; X-ray diffraction

☆ For Part 11, see Ref. [1].

* Corresponding authors. Tel.: +380-622-558-373; fax: +380-622-558-524 (I.F.P.).
E-mail addresses: i_perepichka@yahoo.com (I.F. Perepichka), m.r.bryce@durham.ac.uk (M.R. Bryce).

0022-328X/01/$ - see front matter
PII: S0022-328X(01)00948-2

1. Introduction

Donor–π–acceptor molecules are of great interest for fundamental studies on electronic states and intramolecular charge and electron transfer (ICT, IET) processes in organics, and for materials applications in electronics, optoelectronics, optics, and photonics. Electron acceptors of the fluorene series are known for their ability to increase the photoconductivity of semiconductive polymers and are widely used as sensitisers for hole transport materials [2] and as electron transport materials [3]. Recently, we and other workers studied a number of fluorene acceptors of D–π–A type with ICT from various donor groups (e.g. structures **1a** [4], **1b** and **c** [5], **2** [5a], **3** [1b], **4** [1a,6,7,8], **5** [8], and **6** [9], Chart 1). Particularly, compounds **4** and **5** [7,8,10] are of great interest as photothermoplastic storage media (PSTM) for hologram recording, showing excellent rheological properties and high response of the materials in the ICT region of the acceptors. The 1,3-dithiole unit, which is used as the donor moiety in this family of D–π–A compounds is a known building block for electron donors of the tetrathiafulvalene (TTF) family [11].

Ferrocene itself and its derivatives have been used for the preparation of conductive and magnetic charge transfer complexes [12]. Ferrocene is an electron donor with half-wave potential $E^{1/2}_{ox} = 0.45$ V (vs. Ag | AgCl; acetonitrile, 0.1 M Bu_4NPF_6) comparable to that of TTF (0.34 V under the same conditions) [13,14], and a number of ferrocene–dithiole and ferrocene–TTF hybrid electron donors have been synthesised [13,15,16]. Although in these D^1–π–D^2 diads both donor moieties essentially retain their redox characteristics, recently pronounced intramolecular electronic interactions were observed between two donor moieties for both neutral and charged states [15a].

Ferrocene derivatives have also been exploited intensively in various D–A systems with the aim of studying ICT and IET processes and to design new materials for electronics, NLO optics, photovoltaics, sensors and related applications [17–19]. Thus, Imahori et al. [17] reported push–pull Fc–porphyrin–C_{60} triads for molecule-based artificial photosynthesis, which produce long-lived, charge-separated states with high quantum yields. Since the first report by Green et al. [20] a number of push–pull ferrocene derivatives with high second order NLO response [21] were reported [22,23].

Recently, we synthesised a series of Fc–π–fluorene compounds and demonstrated high first order hyperpolarisabilities for extended π-linkers [24]. To study in more detail the ICT, redox behaviour and solid state structures in this class of donor–acceptor systems we report here the synthesis and properties of nitrofluorene–metallocene (NF, Mc) compounds NF–π–Fc (**8** and **11**) and NF–π–Mc–π–NF (**9** and **10**) (Mc is Fc or Rc) having a short methine fragment (=CH–) as a π-linker. We also report on vinylogues NF–π–Fc (**12**) with the extended π-linker =CH–(CH=CH)$_2$–.

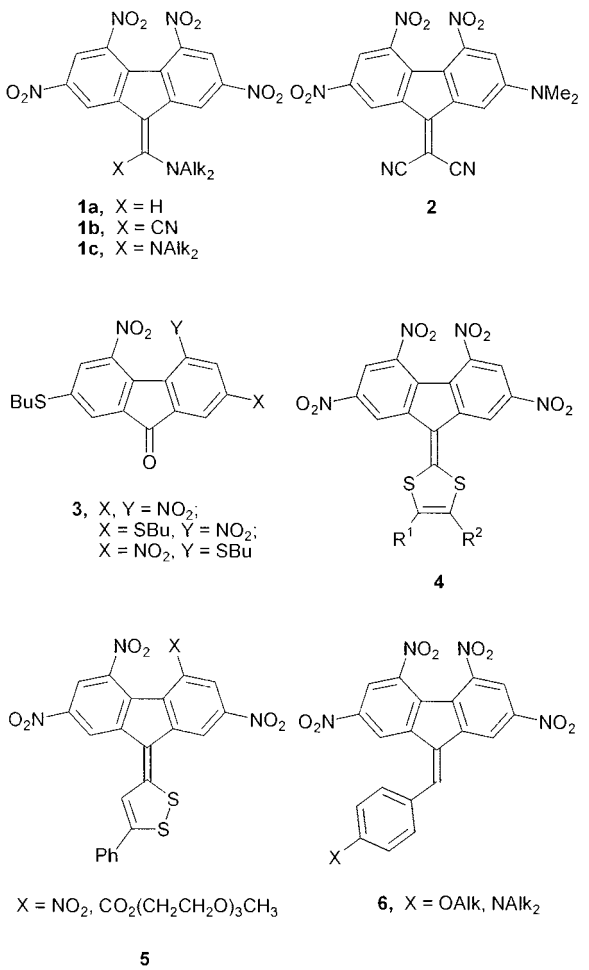

Chart 1.

2. Results and discussion

2.1. Synthesis

The donor–acceptor compounds **8**–**12** have been synthesised by the condensation of the fluorenes **7a**–**g** with the corresponding aldehydes **13**–**16** in *N*,*N*-dimethylformamide (DMF) solution (Scheme 1), applying our established method [7,8,9,24b]. The reaction rate and the yields decrease significantly with a decreasing number of electron withdrawing substituents on the fluorene nucleus (from 0.5 h/20 °C/85% yield for **8a** to 15 h/70 °C/25% yield for **8g**). 4-Cyanofluorene was converted to 9-(ferrocenylmethylideno)-4-cyanofluorene (**8h**) via the lithium salt, followed by coupling with ferrocenecarboxaldehyde. The reaction of ferrocenedi-

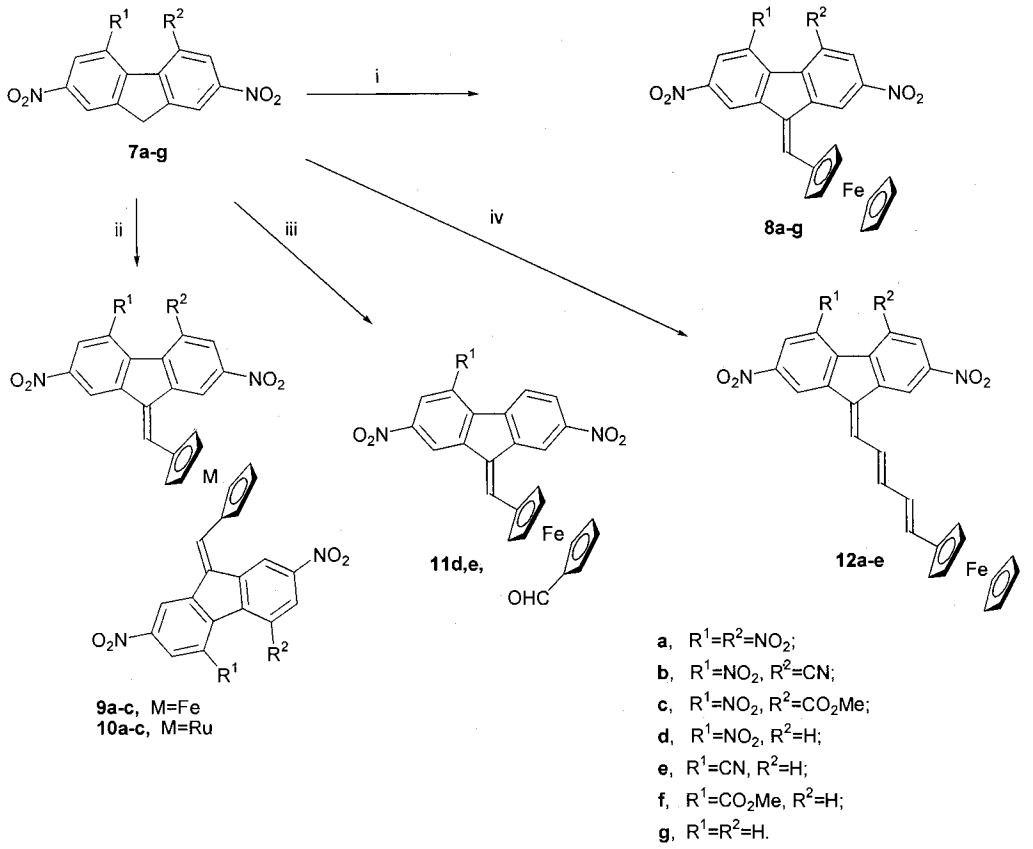

Scheme 1. Reagents and conditions: (i) Ferrocenecarboxaldehyde **13**, DMF, 20–75 °C, 0.5–22 h; (ii) metallocene–1,1′-dicarboxaldehyde **14** or **15**, DMF, 20–60 °C, 1–20 h; (iii) ferrocene–1,1′-dicarboxaldehyde **14**, DMF, 45–60 °C, 20 h; (iv) (*E*,*E*)-1-ferrocenyl-4-formyl-1,3-butadiene **16**, 20–70 °C, 6–25 h.

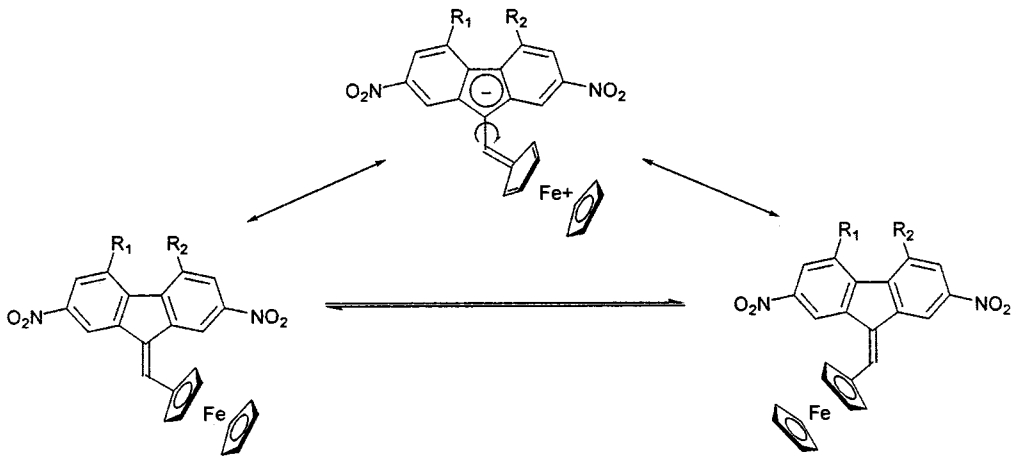

Scheme 2. Lowering the barrier of rotation in compounds **8** through ICT.

carboxaldehyde **14** even with an excess of the relatively poor CH-acidic fluorenes **7d**,**e** gave the mono-adducts **11d**,**e** as the only isolable products. In the case of an unsymmetrical structure of the fluorene moiety ($R^1 \neq R^2$) compounds **8**–**12** were isolated as mixtures of *E* and *Z* isomers (according to their ^{1}H-NMR spectra, Table 1). The isomers could not be separated by chromatography, but pure *E* isomer was isolated for compound **8b** by crystallisation from DMF–acetone solution of the *E*–*Z* mixture.

Table 1
^{1}H-NMR spectral data for fluorenes **8**–**12**

Compound	14-H	1-H ($J_{1,3}$, Hz)	8-H ($J_{6,8,}$ Hz)	3-H	6-H ($J_{6,5}$, Hz)	5-H	$-H_2C_5H_2$	$-H_2C_5H_2$	C_5H_5	Others
8a [a]	8.99s	9.74d (2)	9.50d (2)	8.86d (2)			5.20m	5.09m	4.46s	–
8b [a]	8.90s	*E*: 9.70d (2) *Z*: 9.45d (2)	*E*: 9.42d (2) *Z*: 9.69d (2)	*E*: 8.840d *Z*: 8.82d	*E*: 8.835d *Z*: 8.80d	–	5.17m	5.05m	4.45s	–
8c [a]	8.76s	*E*: 9.65d (2) *Z*: 9.37d (2)	*E*: 9.26d (2) *Z*: 9.56d (2)	*E*: 8.783d *Z*: 8.780d	*E*: 8.631d *Z*: 8.628d	–	5.12m	4.99m	*E*: 4.429s *Z*: 4.427s	3.97s (3H, Me)
8d [a]	8.67s	*E*: 9.62d (2) *Z*: 9.34d (2)	*E*: 9.08d (2) *Z*: 9.45d (2)	*E*: 8.67d *Z*: 8.84d	*E*: 8.43dd (9) *Z*: 8.41dd (9)	*E*: 8.23d *Z*: 8.31d	5.10m	4.93m	*E*: 4.431s *Z*: 4.426s	–
8e [a]	8.62s	*E*: 9.58d (2) *Z*: 9.29d (2)	*E*: 9.09d (2) *Z*: 9.44d (2)	*E*: 8.65d *Z*: 8.79d	*E*: 8.56dd *Z*: 8.53dd	*E*: 8.78d *Z*: 8.75d	5.08m	4.91m	*E*: 4.422s *Z*: 4.417s	–
8f [a]	8.47s	*E*: 9.47d (2) *Z*: 9.14d (2)	*E*: 8.98d (2) *Z*: 9.35d (2)	*E*: 8.68d *Z*: 8.70d	*E*: 8.33dd (9) *Z*: 8.34dd (9)	*E*: 8.63d *Z*: 8.71d	5.02m	4.85m	*E*: 4.402s *Z*: 4.339s	4.16s (3H, Me)
8g [b]	7.84s	9.30d (2)	9.73d (2)	8.34dd	8.33dd (8)	4-H: 7.99d 5-H: 7.98d	4.84t (2 Hz)	4.73t (2 Hz)	4.30s	–
8h [c]	(*E*, *Z*): 8.41d (8, 1H), [8.32–8.22m, 8.19–8.13m, (2H)], 7.91d (6, 1H), 7.81t (7, 1H), 7.57–7.48m (2H), 7.47–7.39m (1H)						*E*: 4.79s *Z*: 4.77s	4.62s	4.28s	–
9a [c]	8.41s	9.52br (2)	8.80d (2)	8.65d	8.33d		5.67s	5.20s	–	–
9b [c]	8.33s, 8.27s, 8.26s, 8.22s	9.45–9.41m (2H), [8.76m, 8.74d (2), 8.69m, 8.64d (2), (4H)], [8.48d (2), 8.46d (2), 8.43d (2), 8.41d (2), (2H)]				–	5.49m	5.17m	–	–
9c [c]	[9.45d (2), 9.44d (2), 9.36m, (2H)], [8.64d (2), 8.62d (2), 8.54d (2), 8.53–8.49m, 8.29–8.26m, 8.26–8.22m, 8.04m, (8H)]						5.45m	5.06s	–	3.77s, 3.75s (6H, Me)
10a [c]	7.76s	9.20s	8.70s	8.38s	8.28s	–	5.53s	5.51s	–	–
10b [c]	7.70s, 7.65s, 7.63s, 7.62s	[9.12d, 9.10d, 9.06d, 9.05d, (2H)], [8.76d, 8.75d, 8.73d, 8.70d, (2H)], [8.513d, 8.507d, 8.48d, 8.45d, (2H)], [8.31d, 8.28d, 8.21d, 8.19d, (2H)]				–	5.53–5.41m		–	–
10c [c]	9.19br, 9.11br, 8.59br, 8.41br, 8.32br, 8.31br, 8.22br, 8.19br, 8.11br, 8.10br, 8.05br, 7.72–7.66br.m,						5.49br	5.42br	–	3.76s (6H, Me)
11d [c]	*E*: 7.86s; *Z*: 9.79s	*E*: 9.33d (2) *Z*: 9.10d (2)	*E*: 8.88d (2) *Z*: 9.18d (2)	*E*: 8.75d *Z*: 8.82d	*E*: 8.35dd (9) *Z*: 8.33dd (9)	*E*: 8.22d *Z*: 8.28d	4.99–4.89 (4H, br.m), 4.83 (2H, br.m), 4.72–4.67 (2H)		–	*E*: 9.954s, *Z*: 9.945s (1H, C*H*O)

Table 1 (Continued)

Compound	14-H	1-H ($J_{1,3}$, Hz)	8-H ($J_{6,8,}$ Hz)	3-H	6-H ($J_{6,5}$, Hz)	5-H	$-H_2C_5H_2$	$-H_2C_5H_2$	C_5H_5	Others
11e [c]	*E*: 7.83s; *Z*: 7.56s	*E*: 9.29d (2) *Z*: 9.05d (2)	*E*: 8.88d (2) *Z*: 9.17d (2)	*E*: 8.59d *Z*: 8.63d	*E*: 8.43dd (8) *Z*: 8.41dd (8)	*E*: 8.71d *Z*: 8.73d	4.99–4.89 (4H, br.m), 4.83 (2H, br.m), 4.72–4.67 (2H)		–	*E*: 9.945s, *Z*: 9.933s (1H, C*H*O)
12a [c]	8.63d (12)	9.46br.s	9.28br.s	8.77br.s	8.70br.s	–	4.78s	4.63s	4.24s	6.13br.m (2H), 7.40–7.50br.m (1H), 7.60–7.76m (1H)
12b [d]	7.90d (12)	*E*: 9.22br *Z*: 8.95br	*E*: 8.95br *Z*: 9.22br	*E*: 8.79br *Z*: 8.74br	*E*: 8.67br *Z*: 8.72br	–	4.72s	4.68s	4.31s	6.84–6.98m (1H), 7.13d (1H, 2 Hz), 7.24–7.37m (1H), 7.37–7.50m (1H)
12c [b]	*E*: 7.78d (13) *Z*: 7.76d (13)	*E*: 9.20d (2) *Z*: 8.92d (2)	*E*: 8.85d (2) *Z*: 9.13d (2)	*E*: 8.83d *Z*: 8.77d	*E*: 8.67d *Z*: 8.73d		4.62t (2 Hz)	4.55t (2 Hz)	4.21s	6.83–7.00m (2H), 7.10–7.20m (1H), 7.36–7.52m (1H), [*E*: 3.884s, *Z*: 3.877s (3H, Me)]
12d [b]	*E*: 7.73d (13) *Z*: 7.56d (13)	*E*: 9.17br *Z*: 8.90br	*E*: 9.02br *Z*: 8.77br	*E*: 8.74br *Z*: 8.73br	*E*: 8.34d (9) *Z*: 8.27d (9)	*E*: 8.32d *Z*: 8.20d	4.60s	4.53s	4.21s	6.80–7.00m (2H), 7.06–7.16m (1H), 7.35–7.53m (1H)
12e [b]	7.65–7.75m	*E*: 9.14br *Z*: 8.86br	*E*: 9.01br *Z*: 8.73br	*E*: 8.61br *Z*: 8.56br	*E*: 8.42d *Z*: 8.37d	*E*: 8.76d (8) *Z*: 8.71d (8)	4.60s	4.52s	4.21s	6.80–7.00m (1H), 7.05–7.12m (2H), 7.35–7.50m (1H)

[a] In acetone-d_6.
[b] In $CDCl_3$.
[c] In Me_2SO-d_6.
[d] In $C_2D_2Cl_4$ at 80 °C.

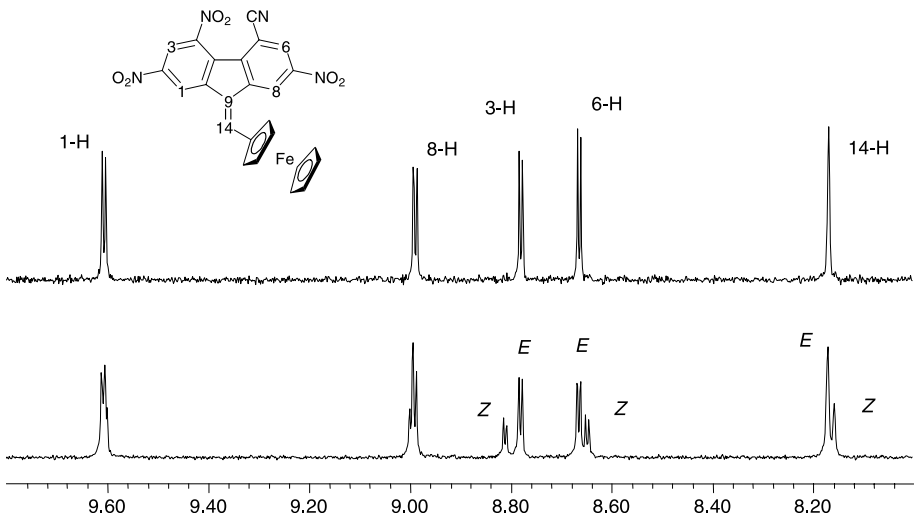

Fig. 1. ^{1}H-NMR monitoring of *E*–*Z* isomerisation of compound **8b** in $CDCl_3$: (top) immediately after dissolution; (bottom) after 4 days storage at 20 °C.

Table 2
CV data for ferroceno–fluorenes **8** (0.2 M $Bu_4N^+PF_6^-$–CH_2Cl_2)

Compound	$E^{1/2}$ (V vs. Fc/Fc^+)				$\Delta E = E^{1/2}_{1red} - E^{1/2}_{2red}$ (V)	EA (eV) [a]
	$E^{1/2}_{1ox}$ ($D \rightarrow D^+$)	$E^{1/2}_{1red}$ ($A \rightarrow A^{\bullet -}$)	$E^{1/2}_{2red}$ ($A^{\bullet -} \rightarrow A^{2-}$)	$E^{1/2}_{3red}$ ($A^{2-} \rightarrow A^{\bullet 3-}$) [b]		
8a	+0.29	−0.93	−1.12	−1.90	0.19	2.10
8b	+0.27	−1.03	−1.17	–	0.14	2.00
8c	+0.30	−1.07	−1.20	–	0.13	1.96
8d	+0.24	−1.21	−1.34	–	0.13	1.82
8e	+0.23	−1.26	−1.32	–	0.06	1.77
8f	+0.21	−1.37		–	–	1.66
8g	+0.19	−1.47		–	–	1.56
8h	+0.12	−2.20		–	–	
*Correlation parameters for **8a–g** using* Eq. (1)						
$E^{1/2}_0$ (V)	0.081 ± 0.019	-2.01 ± 0.03	-1.81 ± 0.04	–		
$\rho_{CV} \times 10^2$ (V)	4.2 ± 0.5	21 ± 1	13 ± 1	–		
$s_0 \times 10^2$	1.8	1.9	2.2			
r	0.961	0.990	0.969	–		

[a] 2,4,5,7-Tetranitro-9-dicyanomethylenefluorene (DTeF) was used as reference acceptor: EA = 2.77 eV, $E^{1/2}_1 = +0.23$ V vs. Ag | AgCl (i.e. −0.26 V vs. Fc/Fc^+) [27].
[b] Quasi-reversible reduction.

2.2. ^{1}H-NMR spectra

Due to the strong ICT in these compounds, which can be represented by zwitterionic resonance structures (Scheme 2), the rotation barrier around the formally double exocyclic C(9)=C(14) bond is expected to be relatively low [5] and *E*–*Z* isomerisation occurs in solution: after 4 days storage of pure (*E*)-**8b** at 20 °C in $CDCl_3$ solution, both isomers were found in a ratio of ca. 2:1 (Fig. 1). The increase in the media polarity significantly facilitates this rotation: a freshly prepared solution of (*E*)-**8b** in acetone showed the presence of both isomers in a 1:1 ratio. Isomerism around two double bonds for **9** and **10** brought about the same complication in their ^{1}H-NMR spectra. For these compounds three isomers can exist in solution: *EE*, *EZ*≡*ZE* and *ZZ*. Taking into account that isomers *EE* and *ZZ* are symmetrical, four sets of signals should be expected [$E_{(EE)}$, $Z_{(ZZ)}$, $E_{(EZ)}$ and $Z_{(EZ)}$], as were observed for derivatives **b** and **c** (where $R^1 \neq R^2$, Table 1).

2.3. Electrochemistry

Due to the presence of both electron acceptor and electron donor moieties in derivatives **8**, in cyclic voltammetry (CV) experiments they display amphoteric redox behaviour involving one fully reversible single-electron oxidation wave, and multistep reduction (re-

versible or partly reversible) processes (Table 2). Although the half-wave oxidation potentials, $E^{1/2}_{ox}$, originating from oxidation of the ferrocene donor show only a minor anodic shift with increasing the number of electron withdrawing substituents on the fluorene ring, the tendency is clear and the value of the shift is statistically reliable (Table 2). For a smaller set of 2,7-disubstituted fluorene–ferrocenes of type **8**, no effect of substituents on the oxidation potentials was reported [25].

In the case of the strongest acceptor, **8a**, three single-electron reduction waves (first two reversible and third quasi-reversible), yielding sequentially the radical anion, dianion and radical trianion species have been observed (Fig. 2, Table 2). However, the kinetic stability of the reduced species thereby obtained is limited,[1] and the redox-response from the decomposition (or rearrangement) products has been observed in the CV.[2]

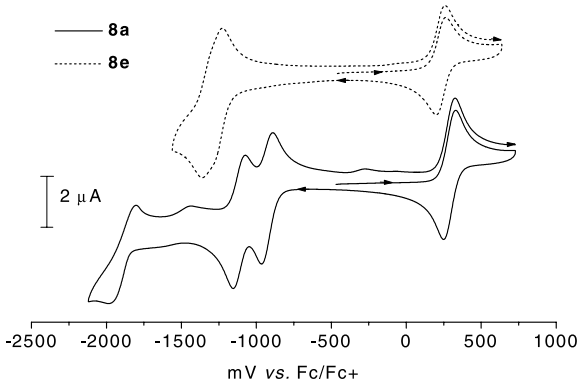

Fig. 2. Cyclic voltammograms of compounds **8a** and **8e** in CH_2Cl_2, electrolyte, Bu_4NPF_6 (0.2 M); scan rate, 200 mV s^{-1}.

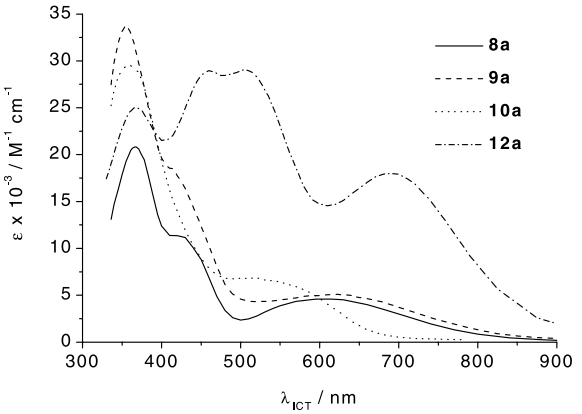

Fig. 3. UV–vis spectra of compounds **8a**, **9a**, **10a** and **12a** in acetone (20 °C).

[1] The instability of the radical anion seems to be a common feature of 9-arylidenofluorenes, which possess a hydrogen atom at the exocyclic double bond. This is in contrast to most other fluorene derivatives without hydrogen at that position.

[2] An increase in the scan rate improved the reversibility of the reduction processes. For **8a** a clear CV has been obtained with the scan rate 1000 mV s^{-1}.

The reduction potentials ($E^{1/2}_{red}$) of the radical anion and dianion formation were found to depend linearly on the nucleophilic σ^-_p constants of the substituents in the fluorene nucleus:

$$E^{1/2} = E^{1/2}_0 + \rho_{cv}\sum\sigma^-_p, \quad (1)$$

where $\Sigma\sigma^-_p$ is the sum of the nucleophilic σ^-_p constants of the substituents [26] in the fluorene nucleus and ρ_{CV} a parameter of the sensitivity of the redox potential to the substituents in the acceptor moiety.

The sensitivity parameters (ρ_{CV}) of the first reduction wave are higher than those of the second one, so the separation between those two waves decreases with a lowering of the electron withdrawing ability of substituents on the fluorene moiety from $\Delta E^{1/2}_{1-2} = 0.19$ V for **8a** to 0.06 V for **8e** (Table 2). This leads to overlapping (Fig. 2, compound **8e**) and then to a complete merger of the first and the second reduction waves, so the reduction of the fluorenes **8f–h** occurs in one two-electron process.

Estimation of electron affinities (EA) of compounds **8a–g** by Eq. (2) [1b,27] characterise them as moderate to weak electron acceptors with EA ranging from 2.10 to 1.56 eV (Table 2):

$$EA(ref) - EA = E^{1/2}_{1red}(ref) - E^{1/2}_{1red} \quad (2)$$

where EA(ref) and $E^{1/2}_{1red}$(ref) are electron affinity and reduction potential for reference acceptor.

The voltammograms for bis-fluorene–metallocenes **9** and **10** were complicated by the presence of two reduction centres (two fluorene moieties), which, together with limited solubility and instability of the reduced species (also for compounds **11** and **12**) precluded an accurate determination of the half-wave reduction potentials for these compounds.

2.4. Electron absorption spectra

The presence of both electron donor and electron acceptor fragments in the compounds under investigation leads to strong ICT which is manifested in the appearance of a long-wavelength absorption bands (ICT band) in the visible region of their electronic spectra (Fig. 3). Its intramolecular nature was established by linear concentration dependence of the absorbances. The maximum of this band, which depends on the metal (Fe, Ru), the substituents on the acceptor moiety, and the solvent used, lie in the range of 500–700 nm (Tables 3 and 4).

The higher donor ability of ferrocene compared to ruthenocene is manifested in a substantially lower ICT energy for compounds **9** (bathochromic shift of $\lambda_{ICT} \approx$ 100 nm from **10** to **9**, Fig. 3). The elongation of the conjugation path between the donor and the acceptor moieties from one to three ethylene linkages also facili-

Table 3
UV–vis spectral data for ferroceno–fluorenes **8**

Solvent (ε^{20}) [a]	$\Sigma\sigma_p^-$	Dioxane (2.21)	Benzene (2.28)	$CHCl_3$ (4.81)	PhCl (5.62)	AcOEt (6.02)	THF (7.39)	CH_2Cl_2 (9.08)	CH_2ClCH_2Cl (10.36)	Acetone (20.74)	MeCN (37.5)
Compound						λ_{ICT} (ε_{ICT})					
8a	5.08	608	615.5	620.5	620.5	609.5	612.5	614	622.5 (4800)	608.5 (4600)	604.5
8b	4.81	598.5	609.5	625.5	621.5	604.5	608	621	627.5	608	609
8c	4.446	589	595.5	603	602.5	591	595.5	603	609	596.5	595
8d	3.81	573.5	582.5	590	588.5	575.5	579.5	588	593.5	578	577.5
8e	3.54	567	574	583.5	580	569	573.5	580.5	586	572	569.5
8f	3.176	558.5	563.5	568	567.5	558.5	562.5	567	571	560.5	559.5
8g	2.54	546	551.5	552.5	552.5	542	547.5	550.5	556	544.5	542
8h	1.00	–	–	–	–	494.5	–	499.5	501	–	–
Correlation parameters for the series ***8*** *using* Eq. (3).											
$h\nu_{ICT}^0$ (eV)		2.51 ± 0.01	2.49 ± 0.01	2.50 ± 0.03	2.50 ± 0.02	2.60 ± 0.02	2.51 ± 0.01	2.55 ± 0.01 [b]	2.56 ± 0.03	2.52 ± 0.02	2.53 ± 0.03
$\rho_{ICT} \times 10^2$ (eV)		-9.1 ± 0.2	-9.4 ± 0.3	-10.2 ± 0.8	-10.1 ± 0.5	-11.4 ± 0.5	-9.6 ± 0.2	-11.2 ± 0.5	-12.0 ± 0.8	-9.8 ± 0.4	-9.9 ± 0.6
$s_0 \times 10^3$		4.1	6.1	17	11	17	4.5	30	27	9.8	14
r		0.999	0.998	0.987	0.994	0.995	0.999	0.989	0.988	0.995	0.990
N		7	7	7	7	8	7	15	8	7	7

[a] Relative permitivities are given in parentheses.

[b] This correlation also includes data for compounds **17a** ($\Sigma\sigma_p^- = 0.25$, $\lambda_{ICT} = 494$ nm), **17b** ($\Sigma\sigma_p^- = 0.27$, $\lambda_{ICT} = 494$ nm), **17c** ($\Sigma\sigma_p^- = 1.27$, $\lambda_{ICT} = 512$ nm), **17d** ($\Sigma\sigma_p^- = 0.50$, $\lambda_{ICT} = 504$ nm), **17e** ($\Sigma\sigma_p^- = 0.54$, $\lambda_{ICT} = 502$ nm), **17f** ($\Sigma\sigma_p^- = 1.03$, $\lambda_{ICT} = 498$ nm) and **17g** ($\Sigma\sigma_p^- = 2.06$, $\lambda_{ICT} = 522$ nm) from Ref. [28].

Table 4
UV–vis spectral data for metalloceno–fluorenes **9**–**12**

Compound	λ_{ICT} (nm) (ε_{ICT} ($M^{-1}\,cm^{-1}$))	
	1,2-Dichloroethane	Acetone
9a	622.5	624 (5100)
9b	610.5	
9c	604	
10a	521.5	508 (6900)
10b	513.5	
10c	499.5	
11d	557	
11e	548	
12a	706	690 (17 000)
12b	692	
12c	663	
12d	638	
12e	625.5	
Correlation parameters for the series ***12*** *using* Eq. (3)		
hv^0_{ICT}/eV	2.51 ± 0.02	
$\rho_{ICT} \times 10^2$/eV	-14.7 ± 0.9	
s_0	0.012	
r	0.994	

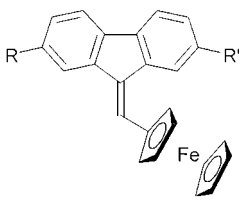

17a, R = H, R' = Br; **17f**, R = H, R' = CHO;
17b, R = H, R' = I; **17g**, R = R' = CHO;
17c, R = H, R' = NO_2; **17h**, R = R' = C≡CH;
17d, R = R' = Br; **17i**, R = R' = C≡CH·$Co_2(CO)_6$;
17e, R = R' = I; **17j**, R = R' = C≡CPt(PEt_3)$_2$Py

Chart 2.

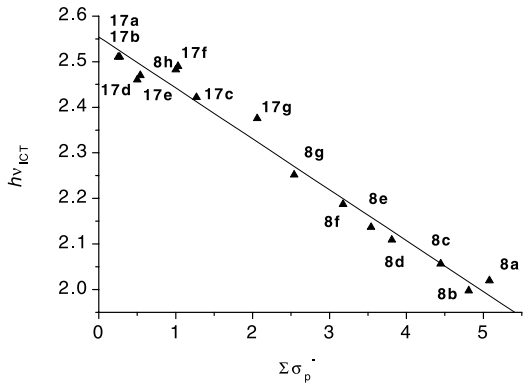

Fig. 4. Correlation between the energy of ICT band (hv_{ICT}) and the sum of nucleophilic constants $\Sigma\sigma_p^-$ of substituents in the fluorene nucleus for series **8** and **17** (CH_2Cl_2, 20 °C). Data for compounds **17** are from Ref. [28] (see Table 3).

tates the ICT process, resulting in a bathochromic shift of ca. 40–80 nm and a significant increase (ca. 3–3.5 times) in the intensity of the ICT band (Fig. 3). Such behaviour is expected for ethylene-bridged conjugated D–π–A systems, and we observed the same tendency in 1,3-dithiole–π–fluorene push–pull chromophores [7a].

Increasing the acceptor character of the fluorene fragment by the introduction of electron withdrawing substituents also results in a bathochromic shift of the ICT band. To estimate quantitatively the effect of the substituents upon the ICT energy (hv_{ICT} corresponding to λ_{ICT}) Eq. (3) [5] was used:

$$hv_{ICT} = hv^0_{ICT} + \rho_{ICT}\sum\sigma_p^- \quad (3)$$

where ρ_{ICT} is a parameter of the sensitivity of ICT energies to the structure of the acceptor moiety.

As seen from Tables 3 and 4, excellent correlations ($r \geq 0.99$) are observed for compounds **8** and **12**. The values of ρ_{ICT} (Tables 3 and 4), are close to those found for the other push–pull fluorene systems reported by us recently [5,7a,b,8b] and only minor variation with the solvent was found for series **8** (between -0.09 and -0.11 eV). The sensitivity parameter for π-extended ferrocenes **12** (-0.15 eV) was somewhat higher than that of the short-bridged compounds **8**.

For compounds of type **8**, data on λ_{ICT} in CH_2Cl_2 are available in the literature for 2,7-substituted 9-ferrocenylidenefluorenes (**17a**–**g**) (Chart 2) [28], and inclusion of literature data into the set shows good linear dependence over the wide range of substituents ($\Sigma\sigma_p^-$ varied from 0.25 for 2-bromofluorene to 5.08 for tetranitrofluorene, Fig. 4).

All the compounds investigated display solvatochromic behaviour (Tables 3 and 4). The maximum observed shift in λ_{ICT} with the change of the solvent (from dioxane to 1,2-dichloroethane) was 26 nm. However, in our case a single parameter, e.g. the medium polarity (ε^{20}) or Reichardt's $E_T(30)$ or E_T^N values [29] is insufficient to describe the solvent effect upon ICT energies, and no satisfactory correlations using the four-parameter Koppel–Palm equation [30] were found.

2.5. Sensitisation of PEPK photoconductivity

Fluorene acceptors are known [1b,2a,b,7a,8c,9,10,31] for their ability to sensitise the photoconductivity of poly-*N*-vinylcarbazole (PVK), poly-*N*-(2,3-epoxypropyl)carbazole (PEPK) and related polymers [32] (Chart 3). Recent studies on photoconductive PEPK films sensitised by fluorene acceptors with ICT show increased photoresponse of the materials in the ICT region of the acceptors [2a,5a,6,7a,9]. The electron affinity of **8a** is close to that for the well-known sensitiser, 2,4,7-trinitrofluorenone (TNF) (Table 2), and its

Table 5
Results of photophysical measurements of PEPK films sensitised by fluorene–ferrocene derivative **8a**

Content of acceptor								
Weight %	Mol %	d (μm) [a]	V_0 (V) [b]	$100\Delta V/V_0$ (%) [c]	$S_{\Delta V}$ ($m^2\ J^{-1}$) [d]	S_η ($m^2\ J^{-1}$) [e]	η_{max} (%) [f]	PM (%) [g]
1.5	0.64	1.4 ± 0.1	200–210	6.0	0.15–0.20	2.0–2.3	8–9	2.5
4.5	1.9	1.5 ± 0.1	210–220	8.0	0.25	2.7–3.0	6–7	2.5
5 [h]	3.1	1.2 ± 0.1	170	10–12	1.4	10–12	20	
3 [i]	1.6	1.2 ± 0.1	140	17–20	3.1	12–13	5–6	

[a] Thickness of the photoconductive film.
[b] Charge potential of the surface of the film in the dark.
[c] Relative dark decay of the surface potential for 30 s.
[d] Electrophotographic response by latent image at the 20% decay level (at $\lambda = 632.9$ nm).
[e] Real holographic response by visualised image at the level of 1% of diffraction efficiency (He–Ne laser, $\lambda = 632.9$ nm).
[f] Maximal diffraction efficiency for plane wave holograms.
[g] 'Parasitic memory', i.e. remained relative diffraction efficiency after erasure.
[h] Data for acceptor TNF from Ref. [31].
[i] Data for acceptor DTeF from Ref. [31].

maximum of λ_{ICT} lies at 604–622 nm (Table 3), which is in the range of radiation of a He–Ne laser ($\lambda = 632.9$ nm), so it seems logical to test acceptor **8a** as a sensitiser for hologram recording. We have studied the electrophotophysical properties of PTSM based on thin films (1.4–1.5 μm) of PEPK sensitised by 1.5 and 4.5 wt.% of acceptor **8a** (concentration was limited by the solubility of the acceptor in the film) using a He–Ne laser as radiation source (Table 5). 'PEPK–**8a**' compositions are good insulators in the dark (the surface can be charged by corona until 140–150 V μm^{-1}), comparable with compositions of PEPK with other fluorene acceptors, and show even lower dark decay of the surface potential ($\Delta V/V_0$) than the known sensitisers TNF and 2,4,5,7-tetranitro-9-dicyanomethylenefluorene (DTeF) (Table 5). However, the photoconductivity is also lower: the electrophotographic response of the materials ($S_{\Delta V}$) is smaller by approximately one order of magnitude. The materials show observable thermorelaxation of the surface potential during thermal development of the latent electrostatic image, so the maximal diffraction efficiency of the holograms (η_{max}) and real holographic response (S_η) have moderate values which allow the recording of holograms with a good quality after amplification of the image. However, these materials are not well suited for hologram recording on a real-time scale, e.g. in holographic interferometry.

2.6. X-ray single-crystal structures

The structures of compounds **8a**, **8g** and **11d** (Figs. 5–7) were determined by single-crystal X-ray diffraction.

The fluorene system in **8a** (Fig. 5) shows the usual [1b,27b,33] distortion, caused by steric repulsion between the nitro groups in positions 4 and 5, which are tilted in opposite directions out of the aromatic plane and 'drag' the C(4) and C(5) atoms with them. Thus, the average displacement of the fluorene carbon atoms from their mean plane is 0.11 Å in **8a**, versus 0.03 Å in **8g** and **11d** (Figs. 6 and 7) where this steric overcrowding is absent. Molecule **11d** (Fig. 7) is disordered. One nitro group is distributed between C(4) and C(5) with the probabilities 64(1) and 36(1)% (this kind of disorder was observed previously in 2,4,7-trinitrofluorene derivatives [34]). Besides this, the nitro group at C(7) is disordered between two positions (A and B), tilted out of the aromatic plane in opposite directions, with occupancies 90(1) and 10(1)%, respectively. The nitro group at C(2) shows a similar disorder (occupancies 64.4(4) and 35.6(4)% for positions A and B), except that here both positions of O(2) coincide, while N(2) and O(1) are disordered. It is likely that the out-of-plane 'tilting' of the last two nitro groups is spurious. In fact, the whole fluorene system may be disordered by rocking in the direction perpendicular to the aromatic plane, but the displacements are too small to be resolved. All the

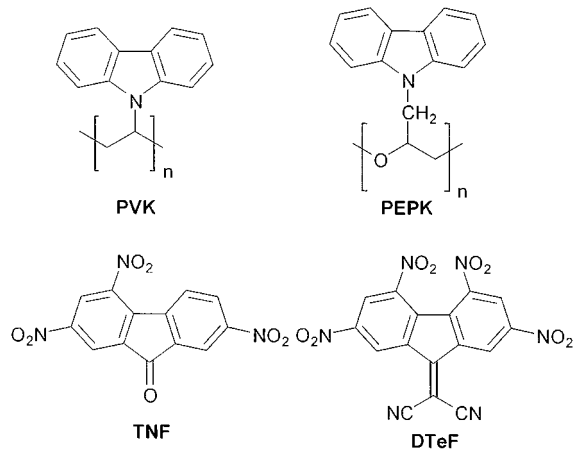

Chart 3.

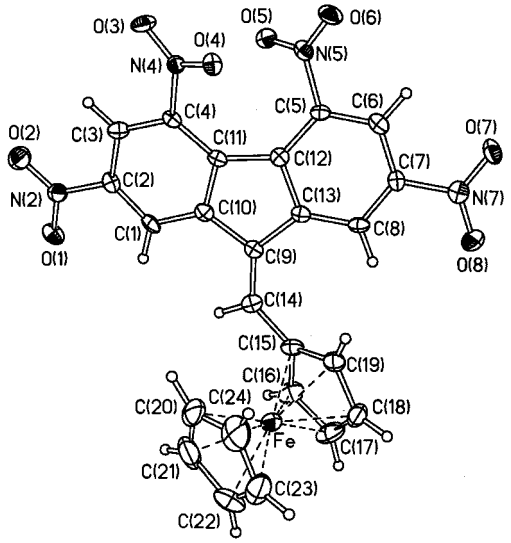

Fig. 5. Molecular structure of **8a**. Henceforth thermal ellipsoids are drawn at 50% probability level.

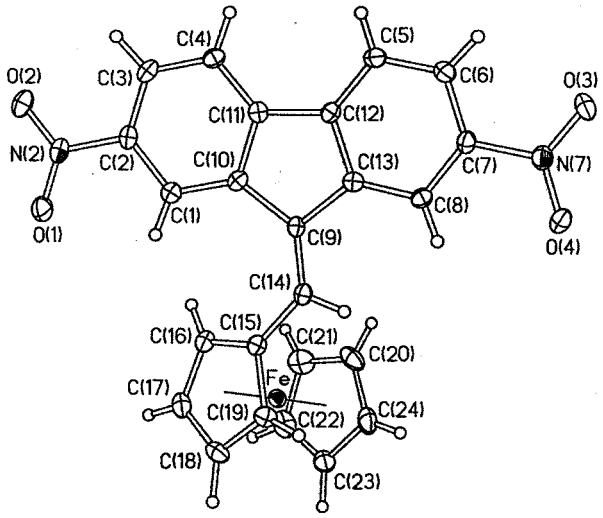

Fig. 6. Molecular structure of **8g**.

carbon atoms of the fluorene moiety have thermal ellipsoids elongated along the perpendicular to its plane, in agreement with this description. Rotation of the nitro groups is generally typical for other fluorene derivatives: for the nitro groups in positions 2 and 7 torsion angles around the C–NO_2 bonds are relatively small with no effects from substitution at positions 4 and 5 (2.3–9.1° for compounds **8a** and **8g**) which is in the range of the literature data (7.4–20° [35]). In **11d** these angles range apparently from 6.8 to 21.8°, although the actual values may be smaller because of the disorder (see above). Positions 4 and 5 have certain steric hindrance and this steric repulsion between the two nitro groups in positions 4 and 5 in **8a** results in their rotation from the plane of the corresponding benzene rings by 29.2 and 40.8° (cf. other 4,5-dinitrofluorene derivatives [1b,27b,33,36]: 26.4–41.7°). Unexpectedly, an even more pronounced rotation of the nitro group in position 4 was observed for compound **11d**, which rotated by 33.0 or 51.2° (for positions A and B, respectively). This is in contrast to expected and generally observed results, where the rotation of 4(5)-nitro groups in 2,4,5,7-tetranitro derivatives is more than in 2,4,7-trinitro derivatives (because of larger steric repulsion), and can be explained by the disorder in the molecule **11d** mentioned above.

Compounds **8a**, **8g** and **11d** display a similar twist between the C(9)=C(14) bond and the adjacent cyclopentadienyl ring, by 26.5(7), 27.6(3) and 29.6(3)°, respectively (Figs. 5–7).

In 2-formyl- and 2,7-diformyl-9-ferrocenylidenefluorenes (**17f,g**) [28], 2,7-diethynyl-9-ferrocenylidenefluorene (**17h**) and its organometallic derivatives **17i,j** [37], this twist is larger (37–40°) and relatively constant, notwithstanding rather different modes of crystal packing. It has been suggested that in NLO vinyl–ferrocene derivatives the planarity of the π-system is stabilised because it facilitates the ICT from the ferrocenyl through the C=C bond of the vinyl group to the electron acceptor substituents at the latter [38]. The less twisted conformation of **8a**, **8g** and **11d** may thus be caused by more electronegative (nitro) substituents. Also, as the number of nitrogroups increases, this should cause stronger delocalisation of π-electron density from the C(9)=C(14) bond and facilitate the twist around this bond.

The precision of the crystal structures is not sufficient to draw an unequivocal conclusion, but the differences in bond lengths (although each of them is on the limit of statistical significance) are all consistent with this description. Thus, the C(9)=C(14) bond in **8a** is longer

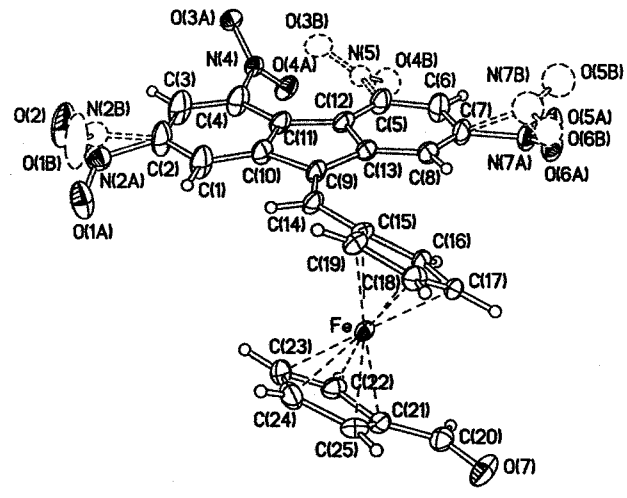

Fig. 7. Molecular structure of **11d**, showing the disorder of nitro groups.

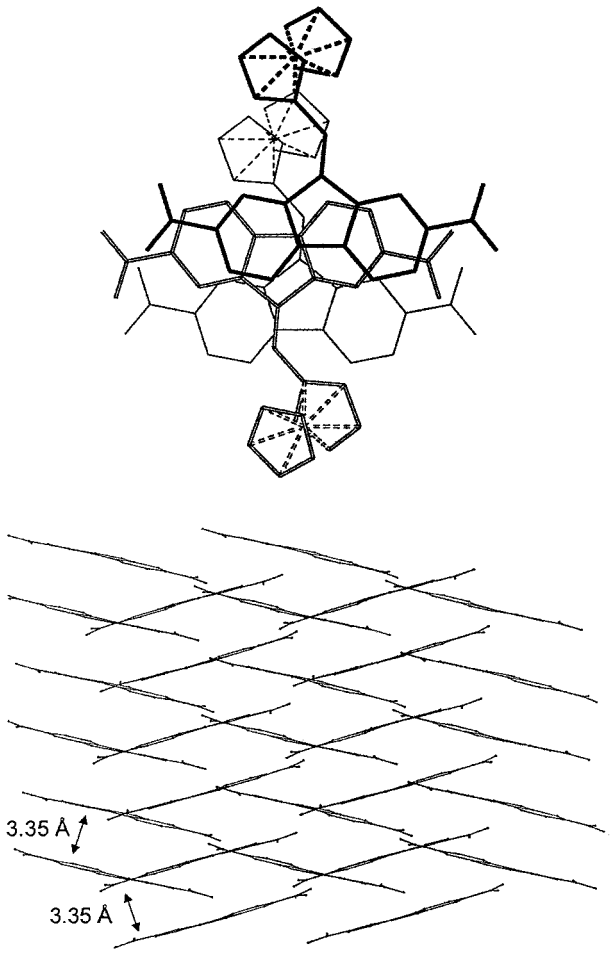

Fig. 8. Molecular overlap (top) and crystal stacks (bottom) showing close-packing pattern of fluorene moieties (ferrocene units omitted for clarity) in compound **8g**.

[1.370(7) Å] than in **8g** and **11d** (1.350(3) and 1.355(5) Å, respectively), while the C(14)–C(15) bond is correspondingly shorter, 1.434(7) Å in **8a** versus 1.453(3) Å in **8g** and 1.455(5) Å in **11d**. Similarly, the C(9)–C(10) and C(9)–C(13) bonds average 1.466(7) in **8a** versus 1.453(3) in **8g** and 1.455(5) in **11d**. More importantly, **8a** displays a significant twist around the C(9)=C(14) bond, 12.6(4) versus 3.3(2)° in **8g** and 5.5(2)° in **11d**. The twist, not warranted by intramolecular steric repulsion, is in accordance with the decreased order of this bond, although in the above mentioned compounds **17f**–**j**, with poor electron accepting properties of fluorene moiety {cf. σ_p^- (NO_2) = 1.27, σ_p^- (CHO) = 1.03, σ_p^- (C≡CH) = 0.53; σ_p (NO_2) = 0.78, σ_p (CHO) = 0.42, σ_p (C≡CH) = 0.23 [26b]}, a twist of 6–9° was also observed [28,37].

The distance between the iron atom and the cyclopentadienyl plane (d) is sensitive to the charge on the ferrocene unit, increasing from 1.649 Å in neutral ferrocene (18-electron configuration of Fc) [39] to 1.702 Å in the 17-electron ferrocenium cation [40]. Therefore, it is noteworthy that the average d in **8a**, **8g** and **11d** increases with the number of nitro groups: 1.648(1) in **8g**, 1.652(2) in **11d**, 1.658(3) in **8a**, although the difference is not statistically significant.

Crystal packing of **8g** and **11d** is similar. Fluorene moieties form stacks, parallel to the x-axis in **8g** and the y-axis in **11d**. Adjacent molecules in a stack are related by inversion centres (Fig. 8, top). The interplanar separations between the average fluorene planes in **8g** are practically uniform along the stack (3.35–3.36 Å) and represent a close-packing pattern (Fig. 8, bottom). In **11d**, these separations alternate between 3.52 and 3.55 Å; closer approach is precluded by the out-of-plane conformation of the nitro groups. The stacks, in their turn, pack in layers, intermingled with layers of ferrocene moieties.

The warped fluorene conformation in **8a** precludes the formation of stacks. Pairs of fluorene moieties contact face-to-face (interplanar distance 3.8 Å) and are surrounded by nitro groups of three other molecules on either outer side. However, this structure is also characterised by alternating layers of fluorene and ferrocene moieties, as are **8g** and **11d**.

3. Conclusions

By reaction of ferrocene caboxaldehyde, its vinylogue, and ferrocene or ruthenocene dicarboxaldehydes with nitrofluorenes, four classes of metallocene–fluorene push–pull compounds of the types Fc–π–fluorene (**8** and **12**), OHC–Fc–π–fluorene (**11**), fluorene–π–Fc–π–fluorene (**9**), and fluorene–π–Rc–π–fluorene (**10**) were synthesised. CV studies showed reversible formation of ferrocenium cation and reversible stepwise single-electron reductions to radical anion and dianion species which merged into one two-electron reduction process with decreasing electron acceptor ability of the fluorene moiety.

The push–pull nature of these compounds resulted in ICT from donor metallocene onto acceptor fluorene fragment, which was monitored by electron absorption spectroscopy. Elongation of the π-bridge (from one π-orbital in **8** to 5 π-orbitals in **12**) results in a bathochromic shift of the ICT band (40–83 nm) and an increase in its intensities. Substitution of Fc in compounds **9a**–**c** by Rc (**10a**–**c**) results in a hypsochromic shift (97–104 nm) of ICT due to lowering the donor ability of the metallocene fragment. Quantitative Hammett-type correlations were obtained for both CV data and ICT energies from spectroscopic data. However, although an observable effect of the solvent was found upon the ICT energies (i.e. for **8a**: λ_{ICT} = 604.5 and 622.5 nm in acetonitrile and 1,2-dichloroethane, respectively) no quantitative relationships were found for a set of 10 solvents.

Moderate ability to sensitise photoconductivity of polymeric semiconductors was demonstrated for acceptor **8a** in the photothermoplastic regime of hologram recording. Determination of molecular and crystal structures for compounds **8a**, **8g**, and **11d** showed π–π stacking of fluorene moieties in compounds **8g** and **11d**. Steric interactions between the nitro groups in positions 4 and 5 of molecule **8a** leads to substantial distortions of the fluorene ring which prevent π–π stack formation. Further studies on ICT process in functionalised fluorene systems, and their applications in molecular electronic devices, are in progress [24b,41].

4. Experimental

4.1. General

^{1}H-NMR spectra were recorded on Varian VXR-400 and UNITY-300 instruments. Chemical shifts, given in ppm, are in relation to Me_4Si as the internal standard. Electron absorption spectra were recorded on a Specord M-40 spectrophotometer. Mass spectra were recorded on a VG7070E spectrometer operating at 70 eV. CV experiments were performed with a PC-controlled BAS CV 50 electrochemical analyser with *iR* compensation. Platinum wire, platinum disk [∅ 1.6 mm (BAS)] and Ag | $AgNO_3$ (in MeCN) were used as counter, working, and quasi-reference electrodes, respectively. In all cases, CV experiments were performed in dry CH_2Cl_2 with $Bu_4N^+PF_6^-$ as the supporting electrolyte (0.2 M) under N_2 flow; concentrations of compounds were ca. 10^{-4} M. The scan rate was 100–1000 mV s^{-1}. All the potentials are given versus ferrocene/ferrocenium (Fc/Fc^+) couple which was used as an internal reference; in our conditions $E^{1/2}$ of Fc/Fc^+ was 0.20 V versus Ag | $AgNO_3$ and 0.49 V versus Ag | AgCl electrodes.

4.2. Ferrocene-1,1′-dicarboxaldehyde (*14*)

Prepared by formylation of 1,1′-dilithioferrocene with DMF according to [42]. ^{1}H-NMR ($CDCl_3$): δ 9.93 (s, 2H, 2CHO), 4.87 (t, 4H, $J = 2$ Hz, $2C_5H_2H_2$), 4.66 (t, 4H, $J = 2$ Hz, $2C_5H_2H_2$).

4.3. Ruthenocene-1,1′-dicarboxaldehyde (*15*)

This was obtained similarly to **14** [43]. ^{1}H-NMR ($CDCl_3$): δ 9.69 (s, 2H, 2CHO), 5.17 (t, 4H, $J = 2$ Hz, $2C_5H_2H_2$), 4.93 (t, 4H, $J = 2$ Hz, $2C_5H_2H_2$).

4.4. 9-(Ferrocenylmethylideno)-2,7-dinitro-4-R^1-5-R^2-fluorenes (*8a–g*). General procedure

Ferrocene carboxaldehyde (93 mg, 0.44 mmol) was added to a solution of fluorene **7a–g** (0.40 mmol) in DMF (1–2 ml) and the mixture was stirred at 20–75 °C until the complete conversion of the starting fluorene (0.5–22 h, TLC monitoring the reaction). The mixture was diluted with 2-propanol (5 ml), left for a few hours at 0–5 °C and the resulting precipitate was filtered off and washed with 2-propanol. The resulting powder (from black to violet colour) was chromatographed on a silica gel column using $CHCl_3$ as the eluent. Deep-coloured fractions containing the product were collected, evaporated under reduced pressure, and the residue was washed with hexane and dried in vacuo, yielding compounds **8a–g**. The reaction time, temperature, yields of the products and the mass spectroscopic and elemental analytical data are summarised in Table 6. ^{1}H-NMR spectra are presented in Table 1.

4.5. 9-[(E)-Ferrocenylmethylideno)-2,4,7-trinitro-5-cyanofluorene ((E)-*8b*)

Compound **8b** (15 mg, mixture of E/Z isomers) was dissolved in warm DMF (0.5 ml), Me_2CO (1 ml) was added and the solution was kept at 0–5 °C for 6 h. The resulting crystalline precipitate was filtered off, washed with Me_2CO and dried in vacuo affording pure (*E*)-**8b** (8 mg, 53%). ^{1}H-NMR ($CDCl_3$); δ 9.61 (d, 1H, $J = 2$ Hz, fluorene 1-H), 8.99 (d, 1H, $J = 2$ Hz, fluorene 8-H), 8.78 (d, 1H, $J = 2$ Hz, fluorene 3-H), 8.67 (d, 1H, $J = 2$ Hz, fluorene 6-H), 8.17 (s, 1H, fluorene=C–*H*), 4.98 (t, 2H, $J = 2$ Hz, Cp), 4.92 (t, 2H, $J = 2$ Hz, Cp), 4.36 (s, 5H, Cp).

4.6. 9-(Ferrocenylmethylideno)-4-cyanofluorene (*8h*)

Butyllithium (1.6 M solution in hexane; 1.5 ml, 2.4 mmol) was added to a solution of di-*iso*-butylamine (262 mg, 2.03 mmol) in dry THF (20 ml) at −78 °C. The solution was allowed to warm to 0 °C for 0.5 h, then it was cooled to −78 °C and 4-cyanofluorene (**7h**) (355 mg, 1.86 mmol) was added, resulting in a deep violet colour. After 10 min, ferrocene carboxaldehyde (450 mg, 2.10 mmol) was added, the reaction mixture was stirred for 3–4 h and the cooling bath was removed. During warming up the mixture turned to dark red. After stirring at 20 °C for 2 h, Et_2O (70 ml) was added, the organic layer was washed with water and brine and dried with K_2CO_3. The solvent was evaporated and the residue was chromatographed on a silica gel column (eluting with $CHCl_3$). Dark red fraction was collected, the solvent was removed under reduced pressure and the resulting product **8h** (365 mg, 55%) was recrystallised from toluene (4 ml), affording pure **8h** (265 mg, 40%) as red crystals, m.p. 185–187 °C. An additional portion of **8h** (70 mg, 10%), m.p. 181–182 °C was obtained by dilution of the mother liquor

with hexane. The mass spectroscopic and elemental analytical data are summarised in Table 6 and the ^{1}H-NMR spectrum is presented in Table 1.

4.7. 1,1′-Bis-(2,7-dinitro-4-R^1-5-R^2-fluoren-9-ylidenmethyl)ferrocenes (**9a–c**). General procedure

Ferrocene-1,1′-dicarboxaldehyde (**14**) (0.2 mmol) was added to a solution of the corresponding fluorene **7** (0.1 mmol) in DMF (2 ml), stirred until full dissolution and the reaction mixture was kept at 20–60 °C for 1–20 h (TLC monitoring the reaction). After storage at 0–5 °C for a few hours the resulting precipitate was filtered off, thoroughly washed with Me_2CO and dried in vacuo at 100–110 °C, yielding products **9a–c** as black powders. The reaction time, temperature, yields of the target products and the mass spectroscopic and elemental analytical data are summarised in Table 6. ^{1}H-NMR spectra are presented in Table 1.

4.8. 1,1′-Bis-(2,7-dinitro-4-R^1-5-R^2-fluoren-9-ylidenmethyl)ruthenocenes (**10a–c**). General procedure

Ruthenocene-1,1′-dicarboxaldehyde (**15**) (0.2 mmol) was added to a solution of the corresponding fluorene **7** (0.1 mmol) in DMF (2 ml), stirred at room tempera-

Table 6
Reaction conditions, yields, m.p.s, MS and elemental analyses for fluorenes **8–12**

Compound	Time (h)	T (°C)	Yield (%)	M.p. (°C)	EIMS: m/z (M^+)	Formula	Found (calc.) (%) or HRMS data		
							C	H	N
8a	0.5	20	85	320 (flash)	542 (100%)	$C_{24}H_{14}N_4O_8Fe$	53.3 (53.2)	2.7 (2.6)	Fe: 10.5 (10.3)
8b	2	20	80	330 (flash)	522 (100%)	$C_{25}H_{14}N_4O_6Fe$	57.15 (57.5)	2.6 (2.7)	10.8 (10.75)
8c	20	20	70	320 (flash)	555 (100%)	$C_{26}H_{17}N_3O_8Fe$	55.9 (56.25)	3.1 (3.1)	7.55 (7.55)
8d	15	50	45	>360	497 (77%), 121 (100%)	$C_{24}H_{15}N_3O_6Fe$	57.55 (57.95)	3.05 (3.05)	8.30 (8.45)
8e	15	60	25	>360	477 (60%), 121 (100%)	$C_{25}H_{15}N_3O_4Fe$	62.7 (62.9)	3.15 (3.15)	8.85 (8.8)
8f	22	65	16	>360	510 (100%)	$C_{26}H_{18}N_2O_6Fe$	61.2 (60.9)	3.6 (3.6)	5.5 (5.5)
8g	15	75	25	330 (dec.)	452 (34%), 392 (100%)	$C_{24}H_{16}N_2O_8Fe$	63.7 (63.3)	3.6 (3.8)	6.2 (6.5)
8h	Individual method		52	185–187	387 (100%)	$C_{25}H_{17}NFe$	77.5 (77.9)	4.4 (4.2)	3.6 (3.8)
9a	1	20	91	365 (flash)	898 (FAB)	$C_{38}H_{18}N_8O_{16Fe}$	50.8 (51.1)	2.0 (1.9)	12.5 (12.7)
9b	10	20	86	>360	858 (FAB)	$C_{40}H_{18}N_8O_{12}Fe$	55.9 (55.7)	2.1 (2.1)	13.1 (13.4)
9c	16	20	70	355 (flash)	924 (FAB)	$C_{42}H_{24}N_6O_{16}Fe$	54.6 (54.9)	2.6 (2.2)	9.1 (9.3)
10a	1	20	74	>360	944 (FAB)	$C_{38}H_{18}N_8O_{16}Ru$	48.4 (48.7)	1.9 (1.9)	11.9 (11.7)
10b	10	20	78	>360	904 (FAB)	$C_{40}H_{18}N_8O_{12}Ru$	53.2 (53.7)	2.0 (2.4)	12.4 (12.1)
10c	90	20	75	350 (flash)	970 (FAB)	$C_{42}H_{24}N_6O_{16}Ru$	52.0 (51.6)	2.5 (2.3)	8.7 (9.0)
11d	20	45	17.5	>360	525 (100%)	$C_{25}H_{15}N_3O_7Fe$	HRMS (EI): 525.02670 (required 525.02594)		
11e	20	60	8.5	>360	505 (100%)	$C_{26}H_{15}N_3O_5Fe$	HRMS (EI): 505.03618 (required 505.03611)		
12a	2	20	97	>300	594 (100%)	$C_{28}H_{18}N_4O_0Fe$	HRMS (EI): 594.04761 (required 594.04740)		
12b	6	20	90	>300	574 (100%)	$C_{29}H_{18}N_4O_6Fe$	HRMS (EI): 574.05617 (required 574.05758)		
12c	12	20	67	>300	607 (6%), 533 (100%)	$C_{30}H_{21}N_3O_8Fe$	59.1 (59.35)	3.50 (3.5)	6.9 (6.9)
12d	15	60	84	>300	549 (100%)	$C_{28}H_{19}N_3O_6Fe$	61.05 (61.2)	3.5 (3.5)	7.75 (7.65)
12e	25	70	10	>300	529 (100%)	$C_{29}H_{19}N_3O_4Fe$	HRMS (EI): 529.07350 (required 529.07250)		

ture (r.t.) for 1–90 h (TLC monitoring the reaction) and diluted with MeOH (1 ml). After storage at 0–5 °C for a few hours the precipitate was filtered off, washed with Me_2CO–MeOH mixture (1:1, v/v) and dried in vacuo at 100–110 °C, affording products **10a–c** as black powders. The reaction time and temperature, yields of the products and the results of mass spectroscopic and elemental analytical data are summarised in the Table 6. ^{1}H-NMR spectra are presented in Table 1.

*4.9. 9-(1′-Formylferrocenyl-1-methylideno)-4-R^1–fluorenes (**11d**,**c**). General procedure*

Ferrocene-1,1′-dicarboxaldehyde (**14**) (0.2 mmol) was added to a solution of the corresponding fluorene **7** (0.1 mmol) in DMF (2 ml), stirred until full dissolution and the mixture was kept at 45–60 °C for 20 h. After storage at 0–5 °C for a few hours the precipitate was filtered off, washed with Me_2CO and dried in vacuo. The crude product contained insoluble impurity; it was purified by extraction with 1,2-dichloroethane in a Soxhlet extractor. The extract was concentrated in vacuo to 0.5–1 ml, the precipitate filtered off and washed with *iso*-octane, affording compounds **11**. The reaction time, temperature, yields of the products and the results of mass spectroscopic and elemental analytical data are summarised in Table 6. ^{1}H-NMR spectra are presented in Table 1.

*4.10. (E,E)-1-Ferrocenyl-4-formyl-1,3-butadiene (**16**)*

Ferrocene carboxaldehyde (**13**) (500 mg, 2.34 mmol) and dry CsF (260 mg, 1.71 mmol) were dissolved in Me_2SO (0.25 ml) and γ-trimethylsilyl-*N*-*tert*-butylcrotonaldimine (from Ref. [44]; now available commercially from Acros) (600 mg, 3.05 mmol) was added at 20 °C. The mixture was stirred for 0.5 h at 20 °C and then for 0.5 h at 100 °C. After cooling to r.t., a degassed solution of $ZnCl_2$ in water (10 ml; 10%) and ether (10 ml) were added (**Caution! A strong exothermic reaction took place during this operation; external cooling is necessary**). The mixture was stirred for 2 h, the organic layer was separated and the water layer was extracted with Et_2O (2×10 ml). The combined Et_2O solutions were washed with brine, dried over $CaCl_2$ and the solvent was removed in vacuo. The residue was chromatographed on silica gel using $CHCl_3$ as the eluent. The first orange fraction of unconverted **25**, was immediately followed by a violet fraction of impure product which was reduced in vacuo to 1–2 ml, diluted with hot hexane (6 ml), filtered while hot and left to crystallise affording violet needles of aldehyde **16** (92 mg, 15%), m.p. 129–131 °C. [The residue after evaporation of the mother liquor contained an additional portion of product **16** (ca. 20 mg, 3%) together with some amount of unconverted ferrocene carboxaldehyde **13**.] EIMS; m/z: 266 [M^+, 100%]. ^{1}H-NMR ($CDCl_3$): δ 9.57 (d, 1H, $J = 8$ Hz, C*H*O), 7.16 (ddd, 1H, $J = 15$, 11 and 0.6 Hz, –CH=CH–C*H*=CH–CHO), 6.89 (d, 1H, $J = 15$ Hz, –C*H*=CH–CH=CH–CHO), 6.60 (ddd, 1H, $J = 15$, 11 and 1 Hz, –CH=C*H*–CH=CH–CHO), 6.15 (ddd, 1H, $J = 15$, 8 and 1 Hz, –CH=CH–CH=C*H*–CHO), 4.50 (t, 2H, $J = 2$ Hz, Cp), 4.43 (t, 2H, $J = 2$ Hz, Cp), 4.16 (s, 1H, Cp). ^{13}C-NMR ($CDCl_3$): δ 193.80 (*C*=O), 152.89, 143.65, 128.88, 123.77, 80.41 (Cp), 70.83 (Cp), 69.70 (Cp), 68.15 (Cp).

*4.11. 1-Ferrocenyl-5-(2,7-dinitro-4-R^1-5-R^2-fluorene-9-ylidene)-1,3-pentadiene (**12a–e**)*

(E,E)-1-Ferrocenyl-4-formyl-1,3-butadiene (**16**) (0.08 mmol) was added to a solution of the corresponding fluorene **7** (0.10 mmol) in DMF (1 ml) and the mixture was stirred at 20–70 °C until full conversion of the starting aldehyde (TLC monitoring the reaction). After cooling, the resulting precipitate was filtered off (except in a case of **12e** when the reaction mixture was first diluted with Me_2CO, 2 ml), washed with DMF (for **12a–d**), then with Me_2CO and dried in vacuo, yielding pure **12** as a black powder. The reaction time, temperature, yield of the product and mass spectroscopic and elemental analytical data are summarised in Table 6. ^{1}H-NMR spectra are presented in Table 1.

4.12. Photophysical measurements of sensitised PEPK films

PTSM were prepared as follows: anionic PEPK (0.5 g) [45] and a corresponding amount of the acceptor were dissolved separately in methyl ethyl ketone (both in 5 ml), and the solutions were combined and filtered. The resulting solution was supported on an ITO coated glass base. The final thickness of the photoconductive films was 1.4–1.5 μm. The surface of the film was charged by positive corona discharge grid until the maximal possible potential which was then measured by the dynamic sonde method. Relative dark decay of the surface potential ($\Delta V \times 100/V_0$) was estimated for the time of 30 s ($\Delta V = V_0 - V_\tau$, where V_τ is the charge potential of the surface in the dark after $\tau = 30$ s). The electrophotographic response ($S_{\Delta V}$, $m^2\,J^{-1}$) was estimated by latent electrostatic image on the level of 20% decay of the initial potential V_0 under the illumination with wavelength of 400–900 nm and the intensity of 0.1 $\mu W\,cm^{-1}$. The real holographic response (S_η, $m^2\,J^{-1}$) was estimated at the level of 1% diffraction efficiency ($\eta = 1\%$) of the visualised image by recording the holograms of the planar light wave at the spatial frequency of $\nu = 450\ mm^{-1}$ with irradiation of a He–Ne laser ($\lambda = 632.9$ nm). Maximal diffraction efficiency, achieved without amplification of the hologram recording (η_{max}, %), was found as the ratio of the beam intensity

Table 7
Crystal data and experimental details

Compound	**8a**	**8g**	**11d**
Formula	$C_{24}H_{14}FeN_4O_8$	$C_{24}H_{16}FeN_2O_4$	$C_{25}H_{15}FeN_3O_7$
Formula weight	542.24	452.24	525.25
Temperature (K)	120	120	100
Crystal system	Monoclinic	Monoclinic	Monoclinic
Space group	$P2_1/c$ (# 14)	$P2_1/c$ (# 14)	$P2_1/c$ (# 14)
Unit cell dimensions			
a (Å)	12.850(6)	7.262(1)	13.418(2)
b (Å)	11.308(5)	10.307(1)	7.258(1)
c (Å)	15.640(7)	25.114(3)	21.624(3)
β (°)	103.76(1)	97.64(1)	91.84(1)
V (Å^3)	2207(2)	1863.1(4)	2104.8(5)
Z	4	4	4
Reflections collected	16836	18834	24605
Unique reflections	3889	4292	5577
R_{int}	0.104	0.052	0.103
Reflections $F^2>2\sigma(F^2)$	2682	3596	4436
$R[F^2>2\sigma(F^2)]$	0.062	0.036	0.068
$wR(F^2)$ (all data)	0.144	0.085	0.158

diffracted into the first order of a diffraction to the intensity of the beam grazed on the hologram, when the ratio of the intensities of the integrated beams was 1:3.

4.13. X-ray single-crystal diffraction

X-ray diffraction experiments were carried out on a SMART 3-circle diffractometer with a 1K CCD area detector, using graphite-monochromated Mo–K_α radiation ($\bar{\lambda}=0.71073$ Å) and a Cryostream (Oxford Cryosystems) open-flow N_2 gas cryostat. A full sphere of reciprocal space was covered by a combination of five sets of ω scans; each set at different φ and/or 2θ angles. For **11d**, absorption correction was performed by numerical integration based on crystal face-indexing (transmission factors 0.759–0.975). The structures were solved by direct methods and refined by full-matrix least-squares against F^2 of all data, using SHELXTL software [46]. Crystal data and experimental details are summarised in Table 7.

5. Supplementary material

Crystallographic data for the structural analysis have been deposited with the Cambridge Crystallographic Data Centre, CCDC nos. 155467, 155468 and 155469 for compounds **8a**, **8g** and **11d**, respectively. Copies of this information may be obtained free of charge from The Director, CCDC, 12 Union Road, Cambridge CB2 1EZ, UK (Fax: +44-1223-336-033; e-mail: deposit@ccdc.cam.ac.uk or www: http://www.ccdc.cam.ac.uk).

Acknowledgements

We thank EPSRC for funding the research in Durham (D.F.P. and A.C.), The Royal Society and The Royal Society of Chemistry (Journals Grant for International Authors) for funding visits to Durham (I.F.P.).

References

[1] (a) Part 11: P.J. Skabara, I.M. Serebryakov, I.F. Perepichka, N.S. Sariciftci, H. Neugebauer, A. Cravino, Macromolecules 34 (2001) 2232;
(b) Part 10: I.F. Perepichka, A.F. Popov, T.V. Orekhova, M.R. Bryce, A.M. Andrievskii, A.S. Batsanov, J. Heaton, J.A.K. Howard, N.I. Sokolov, J. Org. Chem. 65 (2000) 3053.

[2] (a) I.F. Perepichka, in: F. Kajzar, M.V. Agranovich (Eds.), Multiphoton and Light Driven Multielectron Processes in Organics: Materials, Phenomena, Applications. In: NATO Science Series: 3. High Technology, vol. 79, Kluwer Academic, Dordrecht, 2000, p. 371;
(b) N.I. Sokolov, Yu.M. Barabash, L.V. Poperenko, I.F. Perepichka, D.D. Mysyk, V.A. Komarov, Functional Mater. 5 (1998) 441;
(c) I.F. Perepichka, D.D. Mysyk, N.I. Sokolov, in: N.S. Allen, M. Edge, I.R. Bellobono, E. Selli (Eds.), Current Trends in Polymer Photochemistry, Ellis Horwood, New York, 1995, p. 318;
(d) Yu.P. Getmanchuk, N.I. Sokolov, in: Fundamentals of Optical Memory and Medium, vol. 14, Vyscha Shkola, Kiev, 1983, p. 11 (p. 11, in Russian);
(e) H. Hoegl, G. Barchietto, D. Tar, Photochem. Photobiol. 16 (1972) 335.

[3] (a) M. Matsui, K. Fukuyasu, K. Shibata, H. Muramatsu, J. Chem. Soc. Perkin Trans. 2 (1993) 1107;
(b) M. Matsui, K. Shibata, H. Muramatsu, H. Nakazumi, J. Mater. Chem. 6 (1996) 1113.

[4] N.V. Kravchenko, V.N. Abramov, N.M. Semenenko, Zh. Org. Khim. 25 (1989) 1938 (in Russian).

[5] (a) I.F. Perepichka, A.F. Popov, T.V. Orekhova, M.R. Bryce, A.N. Vdovichenko, A.S. Batsanov, L.M. Goldenberg, J.A.K. Howard, N.I. Sokolov, J.L. Megson, J. Chem. Soc. Perkin Trans. 2 (1996) 2453;
(b) I.F. Perepichka, A.F. Popov, T.V. Artyomova, A.N. Vdovichenko, M.R. Bryce, A.S. Batsanov, J.A.K. Howard, J.L. Megson, J. Chem. Soc. Perkin Trans. 2 (1995) 3.

[6] N.G. Kuvshinskii, N.G. Nakhodkin, N.A. Davidenko, A.M. Belonozhko, D.D. Mysyk, Ukr. Fiz. Zh. 34 (1989) 1100.

[7] (a) I.F. Perepichka, D.F. Perepichka, M.R. Bryce, L.M. Goldenberg, L.G. Kuz'mina, A.F. Popov, A. Chesney, A.J. Moore, J.A.K. Howard, N.I. Sokolov, Chem. Commun. (1998) 819;
(b) P.J. Skabara, I.M. Serebryakov, I.F. Perepichka, J. Chem. Soc. Perkin Trans. 2 (1999) 505;
(c) P.J. Skabara, I.M. Serebryakov, I.F. Perepichka, Synth. Met. 102 (1999) 1336.

[8] (a) D.D. Mysyk, I.F. Perepichka, Phosphorus, Sulfur, Silicon 95/96 (1994) 527;
(b) D.D. Mysyk, I.F. Perepichka, D.F. Perepichka, M.R. Bryce, A.F. Popov, L.M. Goldenberg, A.J. Moore, J. Org. Chem. 64 (1999) 6937;
(c) D.F. Perepichka, I.F. Perepichka, M.R. Bryce, A.J. Moore, N.I. Sokolov, Synth. Met. (2001) 1487.

[9] (a) N.M. Semenenko, V.N. Abramov, N.V. Kravchenko, V.S. Trushina, P.G. Buyanovskaya, V.L. Kashina, I.V. Mashkevich, Zh. Obsch. Khim. 55 (1985) 324 (in Russian);

(b) V.N. Abramov, A.M. Andrievskii, N.A. Bodrova, M.S. Borodkina, N.V. Kravchenko, L.I. Kostenko, I.A. Malakhova, E.G. Nikitina, I.G. Orlov, I.F. Perepichka, I.S. Pototskii, N.M. Semenenko, V.S. Trushina. USSR Patent 1,343,760, 1987.

[10] (a) D.D. Mysyk, O.Ya. Neiland, N.G. Kuvshinsky, N.I. Sokolov, L.I. Kostenko, USSR Patent 1,443,366, 1987;
(b) A.M. Belonozhko, N.A. Davidenko, N.G. Kuvshinsky, O.Ya. Neiland, D.D. Mysyk, G.I. Prizva, USSR Patent 1,499,553, 1989;
(c) D.D. Mysyk, O.Ya. Neiland, V.Yu. Khodorkovsky, N.G. Kuvshinsky, A.M. Belonozhko, N.A. Davidenko, USSR Patent 1,665,678, 1991.

[11] M.R. Bryce, J. Mater. Chem. 10 (2000) 589.

[12] (Review on Fc based electronic materials:) A. Togni, in: A. Togni, T. Hayashi (Eds.), Ferrocenes, VCH, Weinheim, 1995, p. 433.

[13] A. Green, M.R. Bryce, A.S. Batsanov, J.A.K. Howard, J. Organomet. Chem. 590 (1999) 180.

[14] S. Hünig, G. Kiesslich, D. Scheutzow, R. Zahradnik, P. Carsky, Int. J. Sulfur Chem. Part C 6 (1971) 109.

[15] (a) S.-G. Liu, I. Perez, N. Martín, L. Echegoyen, J. Org. Chem. 65 (2000) 9092;
(b) D.-Y. Noh, H.-J. Lee, A. Underhill, Synth. Met. 102 (1999) 1698;
(c) H.-J. Lee, D.-Y. Noh, Synth. Met. 102 (1999) 1696.

[16] (a) A.J. Moore, M.R. Bryce, P.J. Skabara, A.S. Batsanov, L.M. Goldenberg, J.A.K. Howard, J. Chem. Soc. Perkin Trans. 1 (1997) 3443;
(b) M.R. Bryce, P.J. Skabara, A.J. Moore, A.S. Batsanov, J.A.K. Howard, V.J. Hoy, Tetrahedron 53 (1997) 17781.

[17] (a) H. Imahori, H. Noreida, H. Yamada, Y. Nishimura, I. Yamazaki, Y. Sakata, S. Fukuzumi, J. Am. Chem. Soc. 123 (2001) 100;
(b) H. Imahori, H. Yamada, Y. Nishimura, I. Yamazaki, Y. Sakata, J. Phys. Chem. B 104 (2000) 2099;
(c) H. Imahori, K. Tamaki, H. Yamada, K. Yamada, Y. Sakata, Y. Nishimura, I. Yamazaki, M. Fujitsuka, O. Ito, Carbon 38 (2000) 1599.

[18] (a) D.T. Gryko, F. Zhao, A.A. Yasseri, K.M. Roth, D.F. Bocian, W.G. Kuhr, J.S. Lindsey, J. Org. Chem. 65 (2000) 7356;
(b) D.M. Guldi, M. Maggini, G. Scorrano, M. Prato, J. Am. Chem. Soc. 119 (1997) 974;
(c) A.K. Burrel, W. Campbell, D.L. Officer, Tetrahedron Lett. 38 (1997) 1249;
(d) R.W. Wagner, P.A. Brown, T.E. Johnson, J.S. Lindsey, J. Chem. Soc. Chem. Commun. (1991) 1463;
(e) J.L. Sessler, M.R. Johnson, S.E. Creager, J.C. Fettinger, J.A. Ibers, J. Am. Chem. Soc. 112 (1990) 9310.

[19] (a) P.D. Beer, S.S. Kurek, J. Organomet. Chem. 366 (1989) C6;
(b) P.D. Beer, S.S. Kurek, J. Organomet. Chem. 336 (1987) C17;
(c) P.D. Beer, M.G. Drew, D. Hesek, R. Jagessar, J. Chem. Soc. Chem. Commun. (1995) 1187.

[20] M.L.H. Green, S.R. Marder, M.E. Thompson, J.A. Bandy, D. Bloor, P.V. Kolinsky, R.J. Jones, Nature (London) 330 (1987) 360.

[21] For recent reviews see:
(a) S. Barlow, S.R. Marder, Chem. Commun. (2000) 1555;
(b) N.J. Long, Angew. Chem. 107 (1995) 37; Angew. Chem. Int. Ed. Engl. 34 (1995) 21, and references therein.

[22] (a) K.N. Jayaprakash, P.C. Ray, I. Matsuoka, M.M. Bhadbhade, V.G. Puranik, P.K. Das, H. Nishihara, A. Sarkar, Organometallics 18 (1999) 3851;
(b) J. Mata, S. Uriel, E. Peris, R. Llusar, S. Houbrechts, A. Persoons, J. Organomet. Chem. 562 (1998) 197;
(c) X.D. Chai, W.S. Yang, R. Lu, Y.W. Cao, N. Lu, Y.S. Jiang, Y.B. Bai, T.J. Li, Supramol. Sci. 5 (1998) 679;
(d) M. Blanchard-Desce, C. Runser, A. Fort, M. Barzoukas, J.-M. Lehn, V. Bloy, V. Alain, Chem. Phys. 199 (1995) 253.

[23] (a) T.M. Gilbert, F.J. Hadley, C.B. Bauer, R.D. Rogers, Organometallics 13 (1994) 2024;
(b) S.R. Marder, J.W. Perry, B.G. Tiemann, Organometallics 10 (1991) 1896;
(c) S.R. Marder, J.E. Sohn, G.D. Stucky (Eds.), Materials for Non-linear Optics: Chemical Perspectives. ACS Symposium Series, vol. 455, American Chemical Society, Washington, DC, 1991.

[24] (a) I.F. Perepichka, D.F. Perepichka, M.R. Bryce, A. Chesney, A.F. Popov, V. Khodorkovsky, G. Meshulam, Z. Kotler, Synth. Met. 102 (1999) 1558;
(b) A.J. Moore, A. Chesney, M.R. Bryce, A.S. Batsanov, J.F. Kelly, J.A.K. Howard, I.F. Perepichka, D.F. Perepichka, G. Meshulam, G. Berkovic, Z. Kotler, R. Mazor, V. Khodorkovsky, Eur. J. Org. Chem. (2001) in press.

[25] P. Zanello, G. Opromolla, F. Fabrizi de Biani, A. Ceccanti, G. Giorgi, Inorg. Chim. Acta 255 (1997) 47.

[26] (a) C. Hansch, A. Leo, Substituent Constants for Correlation Analysis in Chemistry and Biology, Wiley, New York, 1979 (339pp.);
(b) C. Hansch, A. Leo, R.W. Taft, Chem. Rev. 91 (1991) 165.

[27] (a) D.D. Mysyk, I.F. Perepichka, A.S. Edzina, O. Ya. Neilands, Latvian J. Chem. (1991) 727;
(b) I.F. Perepichka, L.G. Kuz'mina, D.F. Perepichka, M.R. Bryce, L.M. Goldenberg, A.F. Popov, J.A.K. Howard, J. Org. Chem. 63 (1998) 6484.

[28] M.E. Wright, B.B. Cochran, Organometallics 2 (1993) 3873.

[29] C. Reichardt, Solvents and Solvent Effects in Organic Chemistry, VCH, Weinheim, 1990 (p. 363).

[30] (a) I.A. Koppel, V.A. Palm, in: N.B. Chapman, J. Shorter (Eds.), Advances in Linear Free Energy Relationships, Plenum Press, London, 1972, p. 203;
(b) V.A. Palm, in: Fundamentals of Quantitative Theory of Organic Reactions, Khimiya, Leningrad, 1977 (p. 109, in Russian).

[31] D.D. Mysyk, I.F. Perepichka, N.I. Sokolov, J. Chem. Soc. Perkin Trans. 2 (1996) 537.

[32] P. Strohriegl, J.V. Grazulevicius, in: H.S. Nalwa (Ed.), Handbook of Organic Conductive Molecules and Polymers, vol. 1, Wiley, Chichester, 1997, p. 553.

[33] I.F. Perepichka, D.F. Perepichka, S.B. Lyubchik, M.R. Bryce, A.S. Batsanov, J.A.K. Howard, J. Chem. Soc. Perkin Trans. 2 (2001) in press.

[34] A.J. Moore, M.R. Bryce, A.S. Batsanov, J.N. Heaton, C.W. Lehmann, J.A.K. Howard, N. Robertson, A.E. Underhill, I.F. Perepichka, J. Mater. Chem. 8 (1998) 1541.

[35] J. Silverman, N.F. Yannoni, J. Phys. Chem. 71 (1967) 1381.

[36] (a) O.V. Semidetko, L.A. Chetkina, V.K. Bel'skii, A.N. Poplavskii, A.M. Andrievskii, K.M. Dyumaev, Zh. Strukt. Khim. 29 (187) (1988) 187 (Chem. Abstr. 109 (1988) 139617u);
(b) O.V. Semidetko, L.A. Chetkina, V.K. Bel'skii, A.N. Poplavskii, A.M. Andrievskii, K.M. Dyumaev, Dokl. Akad. Nauk SSSR 299 (1988) 375 (Chem. Abstr. 111 (1988) 96782r);
(c) O.V. Semidetko, L.A. Chetkina, V.K. Bel'skii, D.D. Mysyk, I.F. Perepichka, A.M. Andrievskii, Zh. Obshch. Khim. 57 (1987) 415 (Chem. Abstr. 108 (1987) 204311k);
(d) L.A. Chetkina, O.V. Semidetko, V.K. Bels'kii, A.N. Sobolev, A.M. Andrievskii, Acta Crystallogr. C 43 (1987) 931;
(e) R.G. Baughman, Acta Crystallogr. C 43 (1987) 933;
(f) L.A. Chetkina, Z.P. Povetyeva, V.K. Bel'skii, B.P. Bespalov, Kristallografiya 30 (1985) 910 (Chem. Abstr. 103 (1985) 204122w);
(g) A.M. Andrievskii, N.G. Grekhova, N.A. Andronova, R.R. Shifrina, V.N. Alexandrov, K.M. Dyumaev, Zh. Org. Khim. 18 (1982) 1961 (Chem. Abstr. 98 (1983) 106926v);

(h) J. Silverman, N.F. Yannoni, A.P. Krukonis, Acta Crystallogr. B 30 (1974) 1474;
(i) D.L. Dorset, A. Hybl, H.L. Ammon, Acta Crystallogr. B 28 (1972) 3122.
[37] (a) W.-Y. Wong, W.-K. Wong, P.R. Raithby, J. Chem. Soc. Dalton Trans. (1998) 2761;
(b) W.-Y. Wong, H.-Y. Lam, S.-M. Lee, J. Organomet. Chem. 595 (2000) 70.
[38] M.E. Wright, E.G. Toplikar, Macromolecules 25 (1992) 6050.
[39] (a) P. Seiler, J.D. Dunnitz, Acta Crystallogr. B 35 (1979) 2020;
(b) P. Seiler, J.D. Dunnitz, Acta Crystallogr. B 38 (1982) 1741.
[40] (a) N.J. Mammano, A. Zalkin, A. Landers, A.L. Rheingold, Inorg. Chem. 16 (1977) 297;
(b) M.R. Churchill, A.G. Landers, A.L. Rheingold, Inorg. Chem. 20 (1981) 849;
(c) S. Pohl, R. Lotz, W. Saak, D. Haase, Angew. Chem. Int. Ed. Engl. 28 (1989) 344.
[41] D.F. Perepichka, M.R. Bryce, E.J.L. McInnes, J.P. Zhao, Org. Lett. 3 (2001) 1431.
[42] G.A. Balavoine, G. Doisneau, T. Fillebeen-Khan, J. Organomet. Chem. 412 (1991) 381.
[43] U.T. Mueller-Westerhoff, Z. Yang, G. Ingram, J. Organomet. Chem. 463 (1993) 163.
[44] M. Bellassoued, M. Salemkour, Tetrahedron 52 (1996) 4607.
[45] J. Inaki, G. Sheibeni, K. Takemoto, Technol. Repts Osaka Univ. 25 (1975) 249.
[46] SHELXTL, Version 5.10, Bruker AXS Inc., Madison, Wisconsin, USA, 1997.